Stability and electronic structure of $B_xN_yC_z$ nanotubes

2006 J. Phys.: Condens. Matter 18 10871

(http://iopscience.iop.org/0953-8984/18/48/014)

INSTITUTE OF PHYSICS PUBLISHING JOURNAL OF PHYSICS: CONDENSED MATTER

J. Phys.: Condens. Matter **18** (2006) 10871–10879 doi:10.1088/0953-8984/18/48/014

Stability and electronic structure of $B_xN_yC_z$ nanotubes

S Azevedo[1], **R de Paiva and J R Kaschny**

Departamento de Física, Universidade Estadual de Feira de Santana, Caixa Postal 252294, 44031-460, Feira de Santana-BA, Brazil

E-mail: sazevedo@uefs.br

Received 10 August 2006, in final form 20 September 2006
Published 17 November 2006
Online at stacks.iop.org/JPhysCM/18/10871

Abstract

We apply a first-principles method, based on the density functional theory, to calculate the structural stability and electronic properties of $B_xN_yC_z$ nanotubes. We follow the evolution of the electronic and structural properties as a function of the composition, atomic structure and nanotube diameter. The results indicate that nanotubes present a large variety of electronic properties, showing a remarkable dependence on these parameters. The formation energy decreases with the tube diameter, D, and has a strong dependence on the tube stoichiometry. Additionally, the results show that the strain energy of the tubes, relative to the corresponding unstrained sheet material, varies as $1/D^n$. For BC_2N the classical strain law ($n = 2$) is clearly obtained. Nevertheless, in the case of BCN, the exact value of n is a matter of discussion.

1. Introduction

Since their discovery in 1991, carbon nanotubes (CNTs) have been a material of a great interest due to their extraordinary structural, mechanical and electrical properties. Such unique properties of CNTs motivate strong efforts related to their synthesis and a wide range of investigations focused on technological applications. The main focus of research in this field is centred on the development of sensors, nanoelectronics and field emission devices.

Based on the analogy between hexagonal boron nitride and graphite, the existence of carbon nanotubes has also prompted the investigation of boron nitride (BN) nanotubes. Shortly after their theoretical prediction in 1994 [1], BN nanotubes were synthesized experimentally in 1995 [2]. However, distinct from their carbon analogues, BN nanotubes are semiconductors characterized by a wide band-gap energy of about 5.5 eV, independent of their radii and helicities [3]. In this field, an interesting possibility arises from the inclusion of substitutional carbon atoms in the BN structure, leading to the formation of ternary $B_xN_yC_z$ compounds with distinct stoichiometries. Some of these compounds have been synthesized experimentally

[1] Author to whom any correspondence should be addressed.

using electric arc-discharge, pyrolysis and mechanical milling of hexagonal BN and graphite powders [4–6]. More recently, aligned BCN nanotubes have been successfully fabricated by bias-assisted hot-filament chemical vapour deposition (CVD) [7, 8].

These developments open up the possibility of producing materials with tunable electronic properties between graphite and boron nitride, suitable to the needs of a specific technological application. This is supported by theoretical calculations, which show that BC_2N nanotubes have a tunable band-gap, intermediate between boron nitride and carbon nanotubes. Moreover, previous studies show that their band-gaps can be controlled by changing their composition and atomic structure. There is a discussion in the literature concerning structural properties of $B_xN_yC_z$ nanotubes and thin films. Some results suggest a partial segregation of C and BN, resulting in a stripe-like or in an island-like configuration [9]. Contrary to these results, other authors suggest a model in which C, B and N atoms are mixed [10, 11]. From the experimental side, it may depend on the synthesis technique where diffusion, solubility and defects can play an important role. In any case, the development of better controlled synthesis processes and the systematic refinement of the theoretical calculations will elucidate these points.

In the present contribution, we apply a first-principles method, based on the density functional theory within the generalized gradient approximation, and the pseudopotential method to investigate the stability and the electronic structure of BCN and BC_2N nanotubes (NTs). We calculate the band-gap, the formation and the strain energies of type (6, 0), (7, 0), (8, 0) and (10, 0) nanotubes, which corresponds to diameters (D) of 4.8, 5.5, 6.3 and 7.8 Å, respectively. The obtained results, as a function of the nanotube diameter, are discussed comparing different compositions and structures.

2. Calculation details

Our calculations are based on the density functional theory [12] as implemented in the SIESTA program [13]. We make use of norm-conserving Troullier–Martins pseudopotentials [14] in the Kleinmann–Bylander factorized form [15] and a double-ζ basis set composed of numerical atomic functions of finite range including polarization orbitals for nitrogen, boron and carbon atoms. For the exchange–correlation potential, we use the generalized gradient approximation (GGA) [16]. All the geometries are fully relaxed, with residual forces smaller than 0.1 eV $Å^{-1}$. Additionally, we adopt the convergence criterion that the self-consistency is achieved when the maximum difference between the output and the input of each element of the density matrix, in a self-consistent field cycle, is about 10^{-4}.

The starting points of our BC_2N and BCN nanotubes are hexagonal plane cells composed of a monolayer of 32 and 24 atoms, respectively. Each unit cell is replicated an integer number of times and attached side by side, forming a stripe. The resulting stripe monolayer is bent to form a tube unit cell. Therefore, the resulting NT diameter, D, is given approximately by πNL, where N is the replication number (an integer) and is L the monolayer length. This procedure is illustrated in figures 1(a)–(d), using the BCN nanotube as an example.

The unit cells of $B_xN_yC_z$ NTs are shown in figures 1 and 2. We considered two different stoichiometries, which are BCN and BC_2N. As mentioned above, figure 1(a) shows the BCN monolayer and figure 1(d) the corresponding NT. As indicated in figures 2(a) and (c), we built two types of BC_2N monolayer with two different atomic arrangements, called model 1 (figure 2(a)) and model 2 (figure 2(c)). The obtained nanotubes are illustrated in figures 2(b) and (d), respectively.

The combination of B, C and N offers a much wider range of possibilities. Theoretical calculations suggest that $B_xN_yC_z$ may be composed of an infinite parallel chain of C–C and

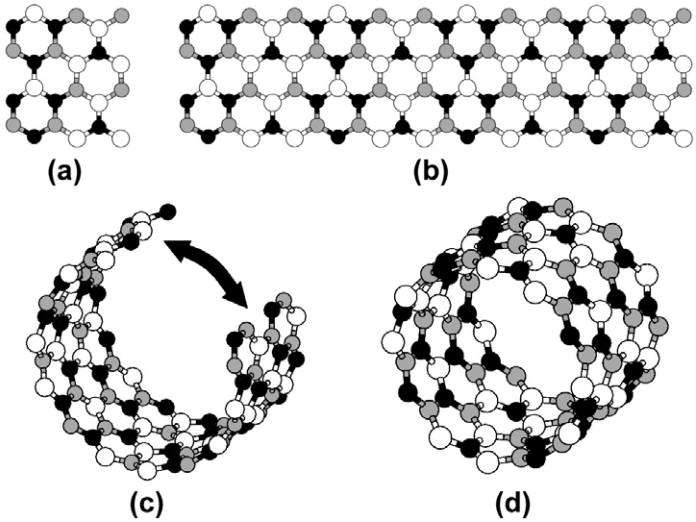

Figure 1. Illustration of the process used to form a BCN nanostructure: (a) starting plane monolayer cell, (b) side by side cell replication forming a stripe, (c) bending process and (d) nanotube formation. Open circles (○) represent B atoms, dark circles (●) N atoms and grey circles (●) the C atoms.

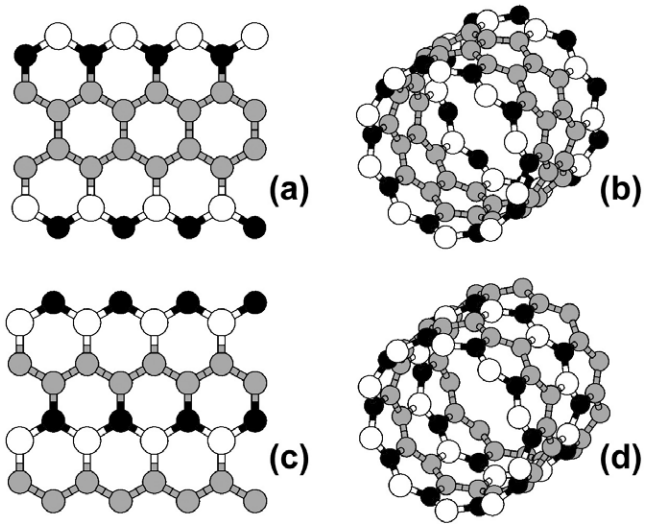

Figure 2. BC_2N nanostructures: (a) model 1 monolayer cell, (b) an example of the obtained model 1 nanotube, (c) model 2 monolayer cell and (d) an example of the obtained model 2 nanotube. Open circles (○) represent B atoms, dark circles (●) N atoms and grey circles (●) the C atoms.

B–N bonds. Such a structure is obtained by using the most stable configuration, under the constraint that the unit cell should contain 8 [17–19], 16 [3] or 32 atoms [20]. Based on this model, where the atomic arrangements are more favourable to form a hexagonal BCN layer, the stability and electronic properties of $B_xN_yC_z$ NTs are studied.

3. Results and discussions

3.1. Relative stability

We now proceed to a comparative analysis of the energetic stability of the structures shown in figures 1 and 2, using a zero-temperature thermodynamic approach based on the prior determination of the chemical potentials [21, 22]. For this purpose, we introduce the calculated chemical potential μ_{BN}, μ_{CC}, for BN and CC pairs, respectively. The chemical potential, $\mu_{BN}^{tube} = -350.17$ eV, is obtained for a BN pair in an infinite zigzag BN single-walled NT (SWNT). Similar to the BN pair, the chemical potential for a CC pair is obtained from a carbon SWNT calculation, which results in $\mu_{CC}^{tube} = -309.72$ eV. Therefore, the formation energy of the nanotubes can be written as

$$E_{form} = E_{tot} - n_B\mu_B - n_N\mu_N - n_C\mu_C, \tag{1}$$

where E_{tot} is the calculated total energy of the nanotube, n_B and n_N and n_C are the number of B, N and C atoms, respectively. Note that the reference energy is taken to be equal to the complete segregation limit, i.e. the C_2 and BN dimer energy in pure carbon and boron-nitride nanotubes.

Using the thermodynamic constraints

$$\mu_N + \mu_B = \mu_{BN}^{tube}, \tag{2}$$

$$\mu_C + \mu_C = \mu_{CC}^{tube}, \tag{3}$$

and assuming that $n_{BN} = n_{CC} = n$ for BC_2N compounds, the equation (1) can be rewritten as

$$E_{form} = E_{tot} - n\left(\mu_{BN}^{tube} + \mu_{CC}^{tube}\right), \tag{4}$$

where n is the number of BN and CC pairs in the unit cell of a BC_2N SWNT.

For the BCN nanotubes, we have

$$E_{form} = E_{tot} - N_{BN}\left(\mu_{BN}^{tube} + \tfrac{1}{2}\mu_{CC}^{tube}\right), \tag{5}$$

where N_{BN} is the number of BN pairs in the unit cell of a BCN SWNT.

The results obtained for the formation energy of $B_xN_yC_z$ NTs, using the above procedure, are summarized in table 1 as a function of the tube diameter, D, where $D = \infty$ corresponds to the plane monolayer. The underlined values in table 1 indicate the most stable structures for each BC_2N model and for BCN. Analysing these results, considering first structures with the same diameter, we find that the model 1 BC_2N nanotube, which has the maximum number of C–C and B–N bonds, is the most stable one. As shown in figure 2(a), such a configuration alternates one B–N chain with two C–C chains, in a so-called stripe-like pattern. Therefore, it is possible that some sort of phase segregation occurs in the most stable structures of BC_2N. This could occur since B and N aggregate alternately, forming BN regions. Then, carbon atoms could segregate from B and N atoms forming graphite-like structures. If such a phase segregation occurs, the number of C–C and B–N bonds increases and the number of B–B and N–N bonds decreases, lowering the formation energy. This result agrees with the previous results of [3]. Additionally, it is also possible to verify that, among all investigated structures, the BC_2N phase is more stable than the BCN ones. This is mainly due to the fact that BC_2N compounds display, in general, a large number of C–C and B–N bonds, when compared to BCN compounds.

The dependence of E_{form} on the NT diameter is illustrated in figure 3(a), where the points correspond to data from table 1 and the lines are used to guide the eyes. This figure shows that the formation energy, obtained using equations (4) and (5), systematically decreases with increasing NT diameter. Each curve tends asymptotically to a constant value, E_∞, that

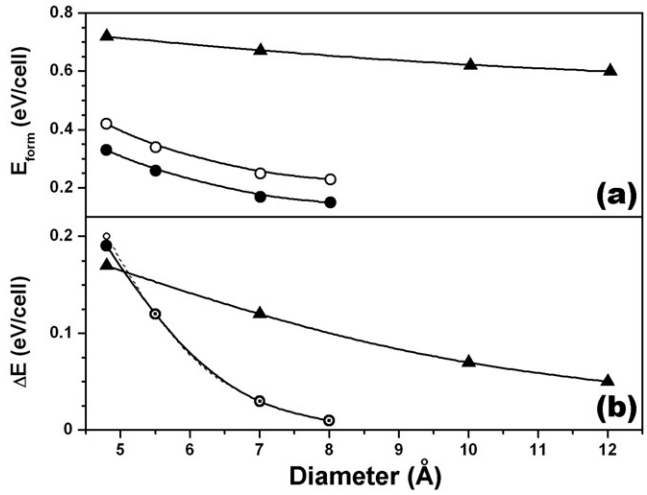

Figure 3. (a) Formation energy, E_{form}, and (b) ΔE plotted as a function of the NT diameter. The dark circles (●) correspond to BC_2N model 1 structure, the open circles (○) to BC_2N model 2 and the dark triangles (▲) to BCN nanotubes. The dot-circles (⊙) indicates the superposition of BC_2N models 1 and 2 data points. The lines are used to guide the eyes.

Table 1. Formation, strain and band-gap energies of boron-carbon-nitride SWNTs. The first column indicates the diameter of each structure, where $D = \infty$ corresponds to the plane monolayer. The second and third column groups indicate the energies of both types of BC_2N NTs. The last column group shows the correspondent energies for BCN NTs. The underlined values indicate the most stable structures for each BC_2N model and for BCN.

	BC_2N model 1			BC_2N model 2			BCN		
D (Å)	E_{form} (eV/cell)	E_{strain} (eV/at.)	E_{gap} (eV)	E_{form} (eV/cell)	E_{strain} (eV/at.)	E_{gap} (eV)	E_{form} (eV/cell)	E_{strain} (eV/at.)	E_{gap} (eV)
4.8	0.33	0.29	—	0.48	0.30	0.03	0.72	0.27	0.10
5.5	0.26	0.22	0.49	0.34	0.22	0.92	—	—	—
7.0	<u>0.17</u>	0.13	1.06	<u>0.25</u>	0.13	1.76	0.67	0.13	0.30
8.0	<u>0.15</u>	0.11	1.28	<u>0.23</u>	0.11	1.57	—	—	—
9.4	—	—	1.18	—	—	1.57	—	—	—
10.0	—	—	—	—	—	—	<u>0.62</u>	0.08	0.30
10.9	—	—	1.13	—	—	1.57	—	—	—
12.0	—	—	—	—	—	—	<u>0.60</u>	0.06	0.30
∞	0.14	—	1.07	0.22	—	1.57	0.55	—	—

corresponds to the formation energy of the plane monolayer, when D tends to ∞. It is clear that the curves for BC_2N models 1 and 2 are very similar. In fact, calculating the energy difference,

$$\Delta E = E_{\text{form}} - E_{\infty}, \tag{6}$$

these curves collapse in the same one, as shown in figure 3(b). Therefore, it is possible to infer that there is a constant difference of about 0.08 eV/cell, exclusively due to the different atomic structures of BC_2N models 2 and 1. Such a difference favours the formation of the stripe-like pattern and confirms that phase segregation should occur in the most stable BC_2N structures. On the other hand, figures 3(a) and (b) make it evident, by direct comparison of

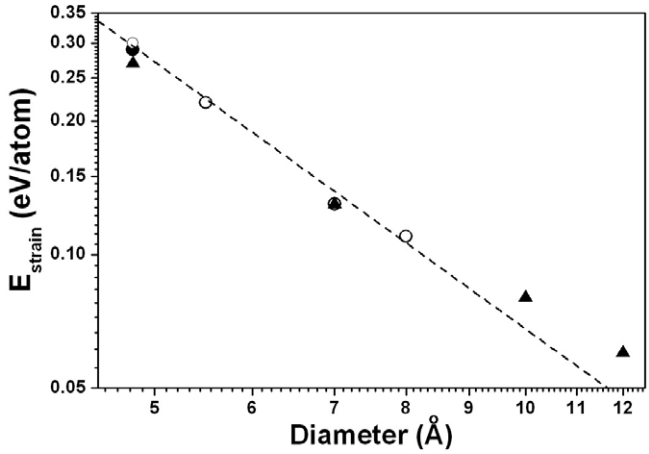

Figure 4. Strain energy plotted as a function of the NT diameter. The dark circles (●) correspond to the BC_2N model 1 structure, the open circles (○) to BC_2N model 2 and the dark triangles (▲) to BCN nanotubes. The dashed line indicates the classical $1/D^2$ law.

BC_2N and BCN curves, that the most important parameter in the NT formation energy is related to stoichiometry.

From the calculation results, it is also possible to obtain the strain energy of BC_2N and BCN NTs. The strain energy per atom, E_{strain}, is defined by:

$$E_{\text{strain}} = E_{\text{tube}} - E_{\text{layer}}, \tag{7}$$

where E_{tube} is the energy per atom of the nanotube and E_{layer} is the energy per atom of the corresponding plane monolayer. The obtained results are summarized in table 1 and plotted in figure 4 (in log × log format) against the NT diameter. It can be observed that we have basically the same strain energies for BC_2N models 1 and 2 NTs, which indicates that the atomic structure does not have strong influence on the strain. In both cases E_{strain} follows a classical $1/D^2$ strain law [23], illustrated by the dashed line in figure 4. Nevertheless, despite the reduced number of data points, it seems that for BCN the strain energy decreases with NT diameter following a $1/D^{1.62}$ law, where the deviation is mainly produced by the data for larger diameters. On average, mixing the BC_2N and BCN results and taking all available data points, the best fit is given by a single curve proportional to $1/D^{1.7}$. On the other hand, considering the possibility that numerical deviations occur during the calculations, it may be reasonable to fit the dependence of BC_2N and BCN strain energy in a single curve using the classical $1/D^2$ strain law.

Additionally, table 2 shows the resulting average bond lengths for each nanotube and the corresponding monolayer. It can be observed that the B–N bond length systematically decreases with the NT diameter for all cases. Despite this, the overall tendency of B–C and C–N bond lengths is not clear and seems to depend on the particular structure. For the BC_2N nanotubes, the average C–C bond length slightly decreases with the tube diameter. In the case of BC_2N model 1 nanotubes, it is possible to divide the C–C bonds in two classes: (i) the bonds parallel to NT axis and (ii) the ones diagonal to this axis. Comparing the average bond length of such classes (see table 2(a)) one can see that, with the exception of the smaller NT diameter, the C–C bonds that are parallel to the NT axis are systematically longer than the other ones.

Table 2. Average bond length of: (a) BC_2N model 1 NTs, (b) BC_2N model 2 NTs, (c) BCN NTs and (d) plane monolayers. See text for additional details.

Diameter (Å)	B–N (Å)	B–C (Å)	C–N (Å)	C–C (Å)	C–C (Å) (parallel)	C–C (Å) (diagonal)
(a)			BC_2N model 1			
4.8	1.467	1.548	1.385	1.444	1.436	1.446
5.5	1.466	1.527	1.394	1.444	1.456	1.441
7.0	1.460	1.529	1.395	1.440	1.453	1.437
8.0	1.459	1.529	1.396	1.439	1.454	1.435
(b)			BC_2N model 2			
4.8	1.463	1.521	1.393	1.448		
5.5	1.457	1.523	1.394	1.442		
7.0	1.452	1.521	1.395	1.437		
8.0	1.451	1.520	1.394	1.437		
(c)			BCN			
4.8	1.464	1.536	1.411			
7.0	1.454	1.526	1.402			
10.0	1.452	1.524	1.401			
12.0	1.444	1.518	1.393			
(d)			Monolayer			
BC_2N model 1	1.455	1.540	1.397	1.441		
BC_2N model 2	1.452	1.535	1.398	1.436		
BCN	1.454	1.526	1.405	—		
BN	1.452	—	—	—		
Carbon	—	—	—	1.461		

3.2. Electronic structure

The obtained results for the energy gap, E_{gap}, of BC_2N and BCN SWNTs are summarized in table 1. It can be observed that the energy gap of BCN NTs, as a function of the tube diameter, grows very fast from 0.1 eV ($D = 4.8$ Å) to the saturation value of about 0.3 eV. It is worth noting that, in general, the CGA underestimates by about 50% the band-gap in comparison with the experimental results. However, even though the CGA-based description is by no means perfect, it presents (as it is a first-principles approach without any phenomenological parameters) a reliable reference point for the analysis of electronic properties of the studied material. A consistent improvement of such results can be achieved only by including the electron correlation in the first-principles calculation, as in Hedin's GW approach [24]. The results obtained with this improvement can be found in [25, 26].

For the case of BC_2N NTs, a more detailed investigation has been carried out including the calculation of E_{gap} for nanotubes with diameters of 9.4 and 10.9 Å. The obtained results are plotted in figure 5 as a function of the tube diameter. The energy gap grows from very small values to a maximum of 1.28 eV, at $D \approx 8$ Å, for BC_2N model 1 and 1.76 eV, at $D \approx 7$ Å, for BC_2N model 2. For larger diameters the results indicate that E_{gap} decreases from such maximum values to the corresponding plane monolayer value, i.e. 1.07 and 1.57 eV, respectively. Such behaviour is consistent with previous results, obtained from first-principles calculations for BC_2N and carbon nanotubes [27, 28], that indicate competition between the size effect and the overlapping of π orbitals. The tube curvature leads to the hybridization of the π orbitals, which is more significant for small tube diameters. Therefore, E_{gap} grows systematically with D due to size effects up to a maximum, with a simultaneous decrease in the

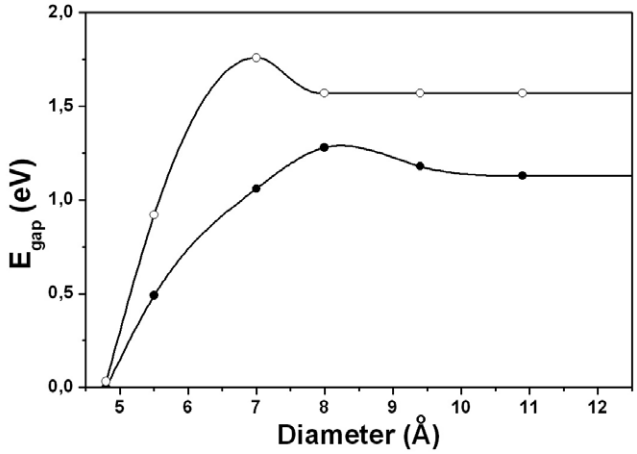

Figure 5. Band-gap energy, E_{gap}, plotted as a function of the NT diameter. The dark circles (●) correspond to the BC_2N model 1 structure and the open circles (○) to BC_2N model 2 nanotubes. The lines are used to guide the eyes.

overlap. After this point the size effect saturates and the overlap remains, decreasing with D leading to smaller E_{gap} values. The energy gap reaches a stable point, about the value for plane monolayer E_{gap}, when the tube diameter is large enough to reduce the curvature hybridization effect to a constant minimum [27].

Additionally, it is possible to observe (see table 1) that the energy gap of BC_2N nanotubes vanishes for small tube diameters, independently of the atomic distribution in the unit cell, reaching a maximum of about 1.8 eV for BC_2N model 2 which is ≈0.5 eV higher than BC_2N model 1. This suggests that BC_2N structures can present quite different electronic and optical properties, varying from metal to semiconductor, depending strongly on tube diameter, with a smaller dependence on the atomic structure of the tube. On the other hand, the energy gap of BCN NTs shows a small variation with tube diameter (from 0.1 to 0.3 eV). Therefore, comparing the results obtained for BCN and BC_2N, it is possible to infer that the electronic structure has a strong dependence on tube stoichiometry.

4. Conclusions

In summary, we investigated the energetic and electronic structure of several infinitely long cylindrical $B_xN_yC_z$ SWNTs using a first-principles calculation. It is shown that compounds with some phase segregation between C and BN (BC_2N) are more stable than nanotubes that display B, C and N (BCN). The calculated strain energy of BC_2N NTs follows a classical $1/D^2$ strain law. Nevertheless, for BCN, some deviation is detected. Concerning electronic structure, the calculations indicate that the energy gap is affected by the stoichiometry, atomic structure and tube diameter. For BC_2N, the dependence of the energy gap on tube curvature is stronger than the dependence on atomic structure of the unit cell. The results suggest competition between the size effect and the overlapping of π orbitals. Comparing the obtained BCN and BC_2N energy gaps, it is possible to observe that BC_2N NTs present a large variety of electronic properties, ranging from metal to semiconductor. Therefore, BC_2N SWNTs may be better candidates for nanosized electronic and photonic device applications.

Acknowledgments

The authors would like to thanks the substantial support given by FAPESB (Fundação de Amparo à Pesquisa do Estado da Bahia—Brazil) and CNPQ (Conselho Nacional de Desenvolvimento Cientifico e Tecnologico—Brazil) during the realization of this work.

References

[1] Rubio A, Corkill J L and Cohen M L 1994 *Phys. Rev.* B **49** 5081
[2] Chopra N G, Luyken R J, Crespi V H, Cohen M L, Louie S G and Zettl A 1995 *Science* **269** 966
[3] Blase X, Rubio A, Louie S G and Cohen M L 1994 *Phys. Rev.* B **51** 6868
[4] Weng-Sieh Z, Cherry K, Chopra N G, Blase X, Miyamoto Y, Rubio A, Cohen M L, Louie S G, Zettl A and Gronsky R 1995 *Phys. Rev.* B **51** 11229
[5] Terrones M, Golberg D, Grobert N, Seeger T, Reyes-Reyes M, Mayne M, Kamalakaran R, Dorozhkin P, Dong Z-C, Terrones H, Rühle M and Bando Y 2003 *Adv. Mater.* **15** 1899
[6] Yao B, Chen W J, Liu L, Ding B Z and Shu W H 1998 *J. Appl. Phys.* **84** 1412
[7] Guo J D, Zhi C Y, Bai X D and Wang E G 2002 *Appl. Phys. Lett.* **80** 124
[8] Yu J, Ahn J, Yoon S F, Zhang Q, Rusli, Gan B, Chew K, Yu M B, Bai X D and Wang E G 2000 *Appl. Phys. Lett.* **77** 1949
[9] Zhang Y, Suenaga K, Colliex C and Iijima S 1998 *Science* **281** 973
[10] Watanabe M O, Itoh S and Mizushima K 1996 *Appl. Phys. Lett.* **68** 2962
[11] Golberg D, Dorozhkin P, Bando Y, Hasegawa M and Dong Z C 2002 *Chem. Phys. Lett.* **359** 220
[12] Kohn W and Sham L J 1965 *Phys. Rev.* A **140** 1133
[13] Sanchez-Portal D, Ordejon P, Artacho E and Soler J M 1997 *Int. J. Quantum Chem.* **65** 453
[14] Troullier N and Martins J L 1991 *Phys. Rev.* B **43** 1993
[15] Kleinman L and Bylander D M 1982 *Phys. Rev. Lett.* **48** 1425
[16] Perdew J P, Burke K and Enrzerhof M 1996 *Phys. Rev. Lett.* **77** 3865
[17] Liu A Y, Wentzcovitch R M and Chen M L 1999 *Phys. Rev.* B **39** 293
[18] Mazzoni M S C, Nunes R W, Azevedo S and Chacham H 2006 *Phys. Rev.* B **73** 73108
[19] Nozaki H and Itoh S 1996 *J. Phys. Chem. Solids* **57** 41
[20] Azevedo S and de Paiva R 2006 *Europhys. Lett.* **75** 126
[21] Alexandre S S, Chacham H and Nunes R W 2001 *Phys. Rev.* B **63** 45402
[22] Azevedo S 2004 *Phys. Lett.* A **325** 283
[23] Robertson D H, Brenner W and Mintmire J W 1992 *Phys. Rev.* B **45** 12592
[24] Aryasetiawan F and Gunnarsson O 1998 *Rep. Prog. Phys.* **61** 237
[25] Blase X 2000 *J. Comput. Mater. Sci.* **17** 107
[26] Blase X, Charlier J C, De Vita A and Car R 1999 *Appl. Phys.* A **68** 293
[27] Pan H, Feng Y P and Lin J Y 2006 *Phys. Rev.* B **73** 35420
[28] Liang W, Wang X J, Yokojima S and Chen G 2000 *J. Am. Chem. Soc.* **122** 11129